Solar Energy Vol. 51, No. 1, pp. 7–18, 1993
Printed in the U.S.A.

0038-092X/93 $6.00 + .00

GEOSTATISTICAL PROPERTIES AND MODELING OF RANDOM CLOUD PATTERNS FOR REAL SKIES

RICHARD PEREZ,* ROBERT SEALS,* JOSEPH MICHALSKY,* and PIERRE INEICHEN**
*Atmospheric Sciences Research Center, State University of New York at Albany, 100 Fuller Road, Albany, NY 12205, U.S.A., **Groupe de Physique Appliquée, University of Geneva, Switzerland

Abstract—A new model that synthesizes sky luminance angular distribution from routine irradiance measurements for all insolation conditions was recently presented by the authors[1]. The model produces continuous sky luminance distribution patterns representative of specific insolation conditions from overcast to clear through partly cloudy. In this article we address the discontinuous aspects of skylight, created by "one of a kind" cloud patterns. We show that these patterns, which are superimposed on the continuous luminance distributions, have predictable physical characteristics that can be parameterized as a function of insolation conditions. We present a method for incorporating these random but predictable luminance effects as an option in the continuous skylight distribution model.

1. INTRODUCTION

Modeling the luminance of the sky for real conditions from routinely available quantities such as solar irradiance is important for two reasons. First, the most recent daylighting design and analysis tools require sky luminance as input[2–4]. Second, actual skylight luminance distribution data are not commonly available.

A recent model evaluation study[1,5]shows that it is possible to adequately model the continuous luminance patterns of real skies and account for such important effects as circumsolar brightening, horizon brightening, or zenith brightening. When evaluated against experimental all-sky scan data, the best models tested exhibit little bias and account well for the prevailing luminances originating from different regions of the sky. However, the root mean square error (RMSE) of these models, that is, their ability to predict the luminance of a particular point in the sky at a particular time, remains high. This is because the modeled luminance patterns, such as the one shown in Fig. 1, do not account for discontinuous effects caused by random cloud distributions. (The sky luminance in Fig. 1 is represented by a grey scale pattern plotted on a three-dimensional "outside" view of the sky hemisphere.) These departures from mean luminance profiles, which at times may be quite pronounced, should be of importance for specific daylighting design issues (e.g., impact on control systems).

It is of course unreasonable to expect that an irradiance-based model will duplicate a particular brightness configuration observed at a given point in time and exhibit no RMS error. However, it is possible to generate random brightness patterns superimposed on the continuous models, which have physical characteristics representative of given insolation conditions. Using a large experimental sky scan data set as support, we address this issue here, by first identifying and then parameterizing these physical characteristics before describing a possible methodology to incorporate these observed features into a user model.

2. PHYSICAL CHARACTERISTICS OF RANDOM BRIGHTNESS PATTERNS

2.1 *Methods*

2.1.1 *Definition of the characteristics of the random sky.* In this article, we will call random brightness pattern, or random sky, that portion of observed luminance distributions that is not explained by the continuous model. Quantitatively, the random sky is defined here as the angular distribution of the ratios (Qvi) between the luminance of a real sky (Lvi), and the luminance of the continuous modeled sky (Lvim), for the corresponding insolation conditions. We will hereafter refer to Qvi as random luminance or as brightness/luminance departure from the modeled continuous sky.

The two characteristics of the random sky that are of interest are:

1. the intensity distribution of Qvi and its variations as a function of insolation conditions; and
2. the spatial distribution of discontinuous features in the sky vault: an important concern is to estimate the angular size of the random patterns in real skies in order to be able to physically recreate meaningful skies where areas of relative brightness inhomogeneities (e.g., clouds) are generally found to be structured in a meaningful pattern and not distributed randomly. A useful statistical tool for delineating such spatial structures is the variogram[6,7]. Experimentally derived variograms are produced to estimate the degree of spatial covariance existing between the random luminance (Qvi) of points in the sky as a function of their angular distance d for different sets of insolation conditions. A sample variogram is presented in Fig. 2 along with a view of the sky hemisphere illustrating the angular distance between sky elements and other solar geometry angles used in this paper.

2.1.2 *Parameterization of insolation conditions.* The parameterization of insolation conditions is identical to that used for our previous models[1,8]. This

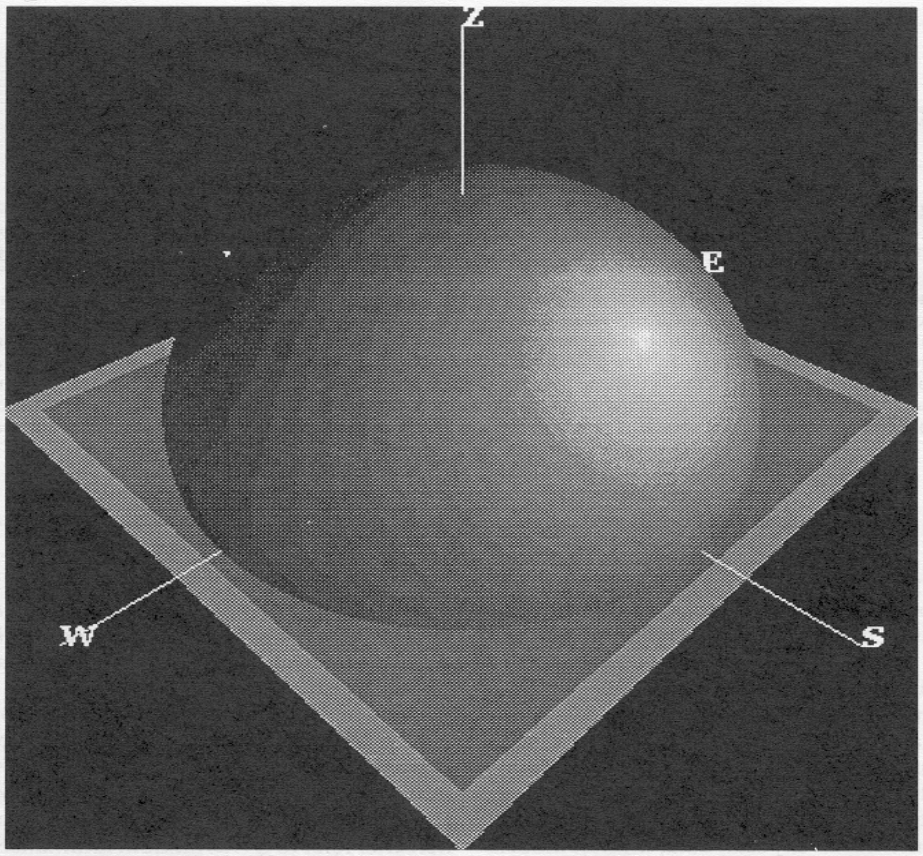

Fig. 1. Example of a modeled continuous sky corresponding to bright overcast conditions. The sky luminance is graphically represented by a grey scale pattern plotted on a 3-D outside view of the sky hemisphere.

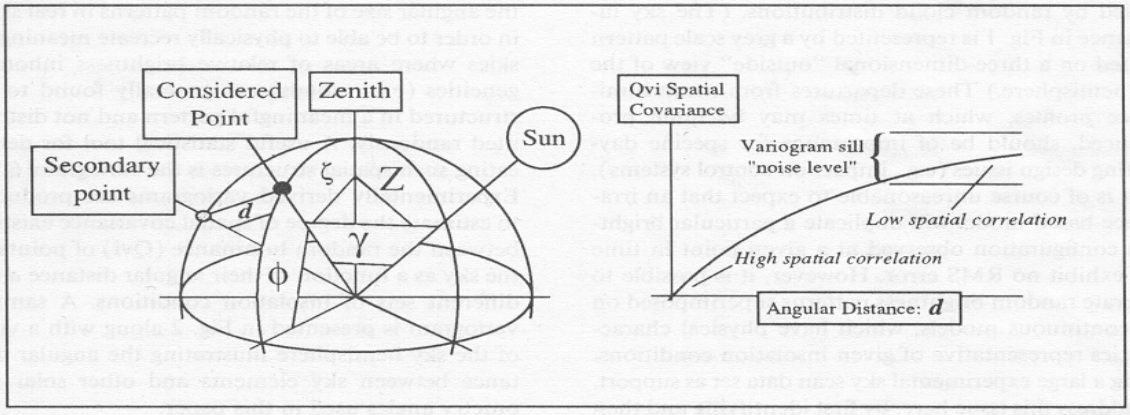

Fig. 2. Illustration of the celestial angles used in this article and of a sample variogram of Qvi as a function of angular distance in the sky vault. d = angular distance between two sky elements. γ = sun's incidence (scattering) angle. ϕ = considered point's elevation. ζ = considered point's zenith angle. Z = solar zenith angle.

parameterization has proven to be largely site-independent. Insolation conditions are delineated with a three-dimensional space, the dimensions of which can be readily derived from routine global and direct (or global only[9]) irradiance data.

The three dimensions are:

1. the solar zenith angle Z;
2. the sky's clearness, $\varepsilon = [(Eed + Ees)/Eed + 1.041Z^3]/[1 + 1.041Z^3]$; and
3. the sky's brightness, $\Delta = m\,Eed/Eeso$

where Eed, Ees, m; and $Eeso$ are the diffuse irradiance, the direct normal irradiance, the optical airmass (e.g., from[10]), and the extraterrestrial normal irradiance, respectively.

For the discontinuous phenomenae studied in this article, we will limit our analysis to two dimensions: the sky clearness and the sky brightness. This is because these *relative* phenomenae should not be *a priori* a function of the position of the sun in the sky. (Although note that, by selecting the parameter Qvi as a measure for nonhomogeneity, we do introduce some solar geometry dependence; however observations show that this effect is not the dominant one and may be neglected, at least for this initial study.)

In this article, we consider 40 insolation condition categories defined by 5 brightness and 8 clearness bins shown in Table 1. The clearness bins are identical to those used in other models developed by Perez *et al.*[8].

Table 1. Gamma function coefficients

		Sky clearness							
	From	1	1.065	1.23	1.5	1.95	2.8	4.5	6.2
	to	1.065	1.23	1.5	1.95	2.8	4.5	6.2	—
Sky brightness									
		Number of observed sky scans (186 data points each)							
From	To								
0	0.1	779							3422
0.1	0.2	1632		7	27	85	1165	2800	1385
0.2	0.3	1614	69	57	95	319	440	24	
0.3	0.4	1012	152	142	148	129	43		
0.4	—	696	142	65	49	50			
		Coefficient *a*							
From	To								
0	0.1	0.3							0.11
0.1	0.2	0.3			0.3	0.3	0.3	0.3	0.11
0.2	0.3	0.3	0.3	0.3	0.3	0.3	0.3	0.3	
0.3	0.4	0.3	0.3	0.3	0.3	0.3	0.3		
0.4	—	0.3	0.3	0.3	0.3	0.3			
		Coefficient *b*							
From	To								
0	0.1	3							125
0.1	0.2	8			6	4	15	47	80
0.2	0.3	8	4	6	6	10	5	27	
0.3	0.4	9	7	15	15	7	6		
0.4	—	19	14	15	12	9			
		Coefficient *c*							
From	To								
0	0.1	0.2400							0.0077
0.1	0.2	0.1080			0.1310	0.1850	0.0610	0.0199	0.0120
0.2	0.3	0.1080	0.1750	0.1300	0.1360	0.0910	0.1460	0.0290	
0.3	0.4	0.1000	0.1280	0.0660	0.0650	0.1290	0.1400		
0.4	—	0.0520	0.0700	0.0690	0.0820	0.1010			
		Coefficient *d*							
From	To								
0	0.1	1							5
0.1	0.2	1			3	2	2	5	3
0.2	0.3	1	3	3	3	2	2	6	
0.3	0.4	2	3	4	4	3	3		
0.4	—	3	3	9	5	3			
		Coefficient *e*							
From	To								
0	0.1	0.5200							0.1780
0.1	0.2	0.5400			0.3200	0.3700	0.3500	0.1750	0.2700
0.2	0.3	0.5400	0.3100	0.2900	0.2640	0.3500	0.4020	0.1970	
0.3	0.4	0.3400	0.2400	0.1920	0.1900	0.2280	0.2740		
0.4	—	0.2200	0.2350	0.0820	0.1350	0.2390			

2.1.3 *The experimental database.* The experimental set of data includes 16,000 all-sky scans recorded in Berkeley, California, between 6/85 and 12/86[11]. Measurements were performed using a multipurpose scanning photometer or MASP developed at Pacific Northwest Laboratory[12]. Each scan consists of 186 samples of luminance across the sky with 10° separation and take about one minute to complete. The data, acquired with a nominal 15 minute time step, include a wide range of insolation conditions from overcast to clear.

Each sky scan consists of 186 individual luminance measurements corresponding to an angular resolution of 10°. This resolution constitutes a limiting factor in our investigation. However, for the considered daylighting applications, this resolution should be more than sufficient[2].

In addition to sky scans we also have time-coincident measurements of direct and global illuminance which allow us (via models, see[1,5]) to parameterize insolation conditions as explained above.

2.2 *Results*

2.2.1 *Intensity distribution of random luminance.* Experimental random luminance distributions were computed, from the entire data set (i.e., 16,000 × 186 data points) for each sky condition category. In Fig. 3, we have illustrated the observed distribution of Qvi for four key sky conditions: dark overcast ($\Delta < 0.1$, $\varepsilon < 1.06$), bright overcast ($\Delta > 0.4$, $\varepsilon < 1.06$), partly cloudy ($0.2 < \Delta < 0.3$, $2.8 < \varepsilon < 4.5$), and clear conditions ($\Delta < 0.1$, $\varepsilon > 6.2$).

As expected, the random sky distributions exhibit the lowest variance for clear conditions. The highest variance is observed for dark overcast skies followed by partly cloudy skies. Bright overcast skies are comparatively more continuous.

We summarized the features of the Qvi distributions with two illustrative benchmarks: (a) their "regularity" which we defined here as the logarithm of the ratio between their kurtosis (or peakedness) and their variance; and (b) their skewness.

In Fig. 4, we have plotted the variations of observed regularity as a function of sky brightness and clearness. The result is a clearly defined pattern with an absolute maximum for very clear conditions (highest ε, lowest Δ), and a relative maximum for bright overcast conditions. Regularity is minimum for dark overcast conditions, and for "extreme" intermediate conditions (extreme = highest and lowest brightness levels for a given clearness). While the absolute maximum for clear conditions was expected, dark overcast conditions

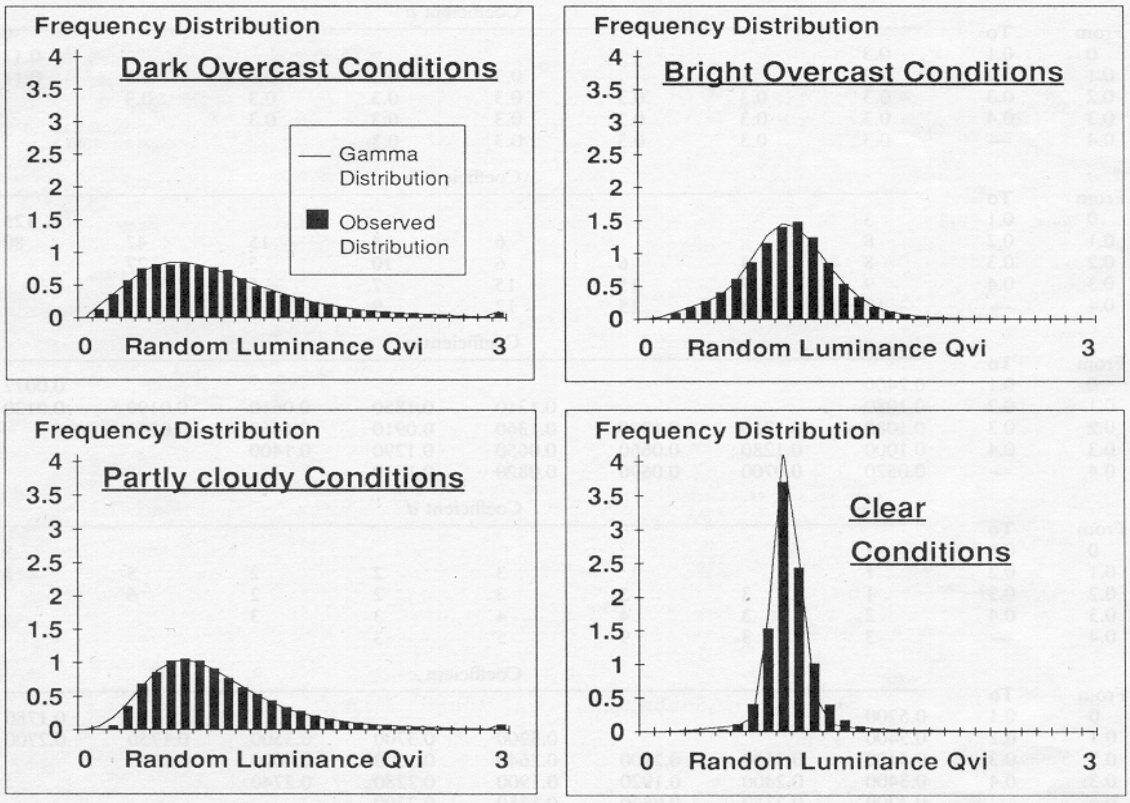

Fig. 3. Frequency distribution of random luminance for selected insolation conditions. The dark columns correspond to experimental observations and the lines corresponded to fitted gamma functions.

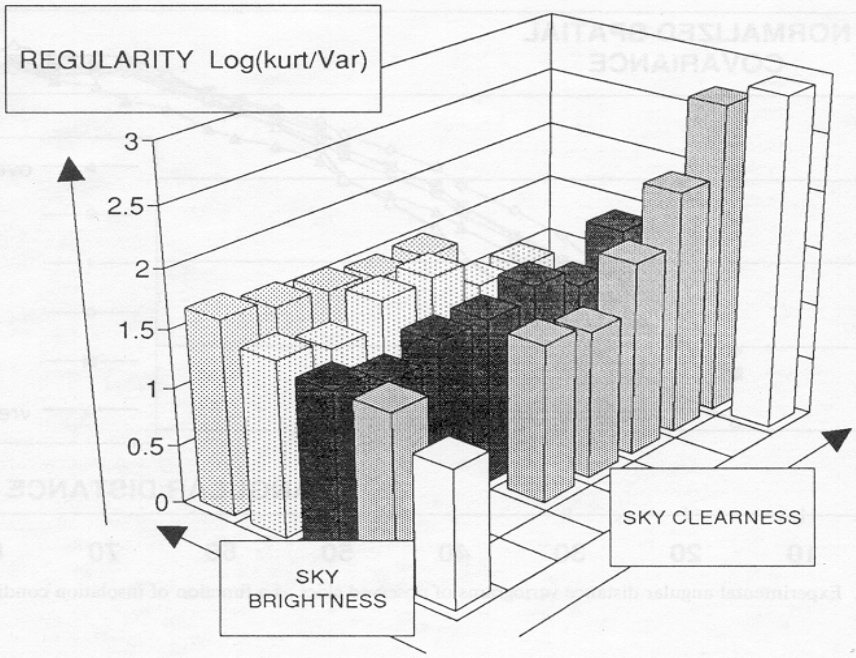

Fig. 4. Regularity of observed skies as a function of insolation conditions.

are not found here to be as continuous as we would have expected from the classical radiative transfer assumptions involving infinite uniform stratus cloud layers[13]. On the other hand, the relative maximum for bright overcast conditions indicates the prevailing presence of uniformly thin layers of clouds. The mid-clearness minima are likely representative of scattered clouds rather than high turbidity conditions (either

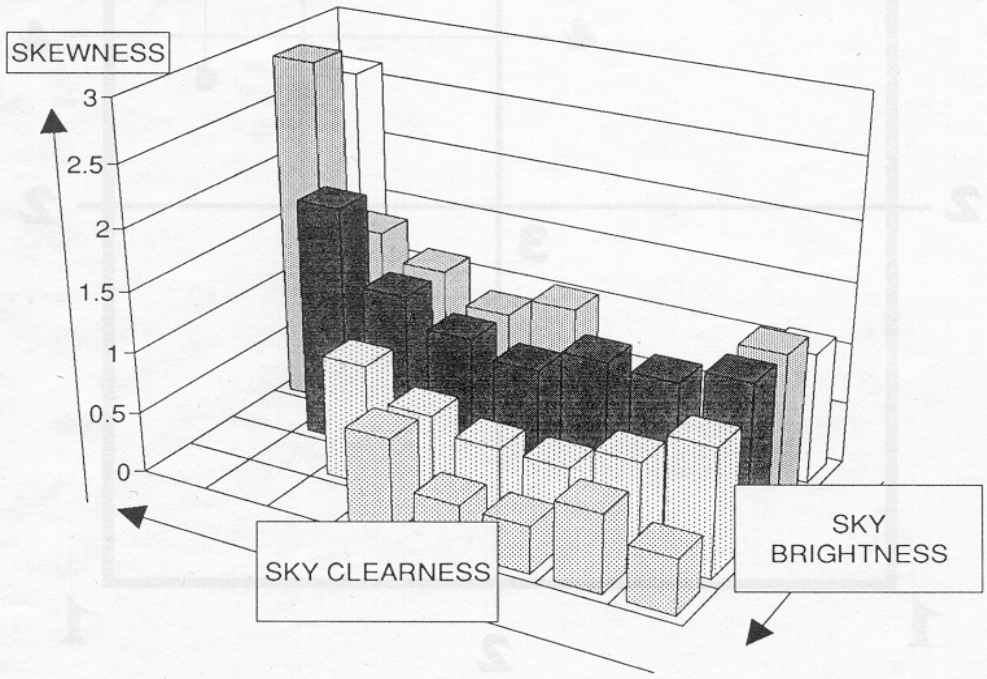

Fig. 5. Skewness of observed random sky distributions as a function of insolation conditions.

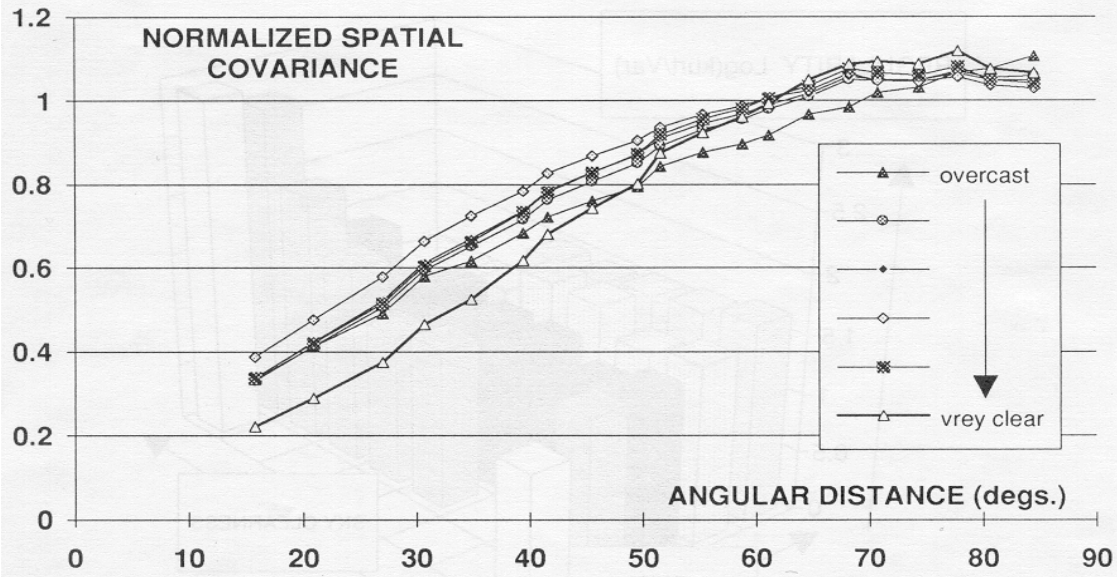

Fig. 6. Experimental angular distance variograms of observed skies as a function of insolation conditions.

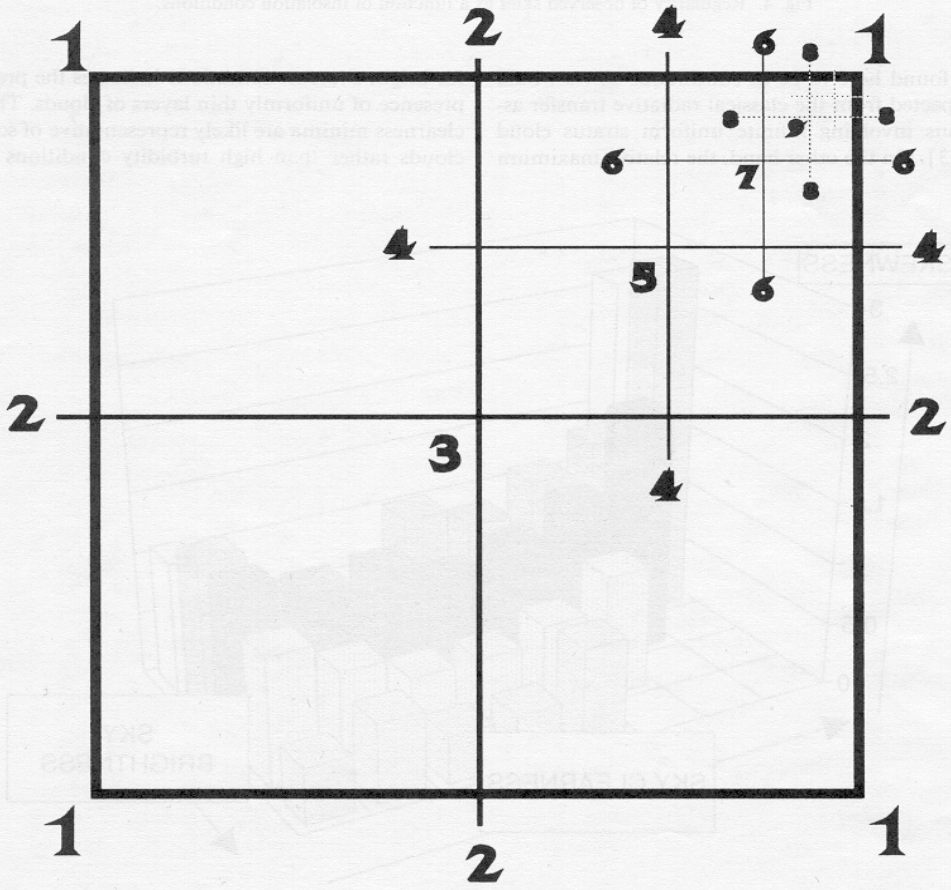

Fig. 7. Schematic of two-dimensional recursive process.

mostly clear with a few clouds or mostly cloudy with a few clear spots).

The variations of the skewness of the Qvi distributions with insolation conditions have been plotted in Fig. 5. Here again, we observe a well defined pattern. Skewness is positive everywhere, which indicates that all distributions have a right-handed asymmetry. However, the degree of asymmetry varies noticeably—and predictably—with insolation conditions. This decreases with brightness and exhibits an absolute maximum for clear conditions. These features may be explained on the following basis: in low brightness skies, the inhomogeneities are likely to be bright patterns on a dark background (e.g., "holes" in a cloud deck), creating a strong right asymmetry; in bright skies, more of the inhomogeneities are likely to be dark spots (e.g., a few thicker clouds), hence a reduced right-handed asymmetry (for instance compare the bright and dark overcast distributions in Fig. 3); for clear skies, inhomogeneities, if any, are likely to be bright spots (e.g., small clouds) on a darker blue sky background, and since these distributions are very narrow (high regularity), only moderate inhomogeneities are sufficient to reach a high skewness.

2.2.2 *Spatial structure of random luminance.* In Fig. 6 we have plotted the experimental spatial variograms of Qvi for insolation conditions ranging from overcast to clear as defined by sky clearness. For the sake of comparison, since the degree of Qvi variance varies considerably from overcast to clear, variograms have all been normalized to their highest variance.

It is recalled that an experimental variogram reports on the observed covariance between points as a function of their distance d (in this case the angular distance of points in the sky, see Fig. 2). This covariance tends toward a minimum at $d = 0$ (this minimum may be non-zero for structures with discontinuous inhomogeneities referred to as "nuggets"[7]) and stabilizes at a maximum "noise" value, referred to as the variogram's sill, beyond a certain range.

For now, we cannot study the behavior of the variograms at very short distances, because of our instrument's limited resolution.

For the angular range studied (i.e., from 15° to 90°), the observed normalized variograms are found to be quite similar for all insolation conditions, with small exceptions for the clear and overcast extremes. (Of course, the non-normalized variograms have different sills for different conditions: very low for clear, highest for overcast and intermediate.)

This insolation condition-independent behavior for the spatial structure of skylight inhomogeneities may appear surprising at first, and this observation will definitely need to be repeated for other sites and/or with higher resolution instruments. However, this result is not inconsistent with the two recent following obser-

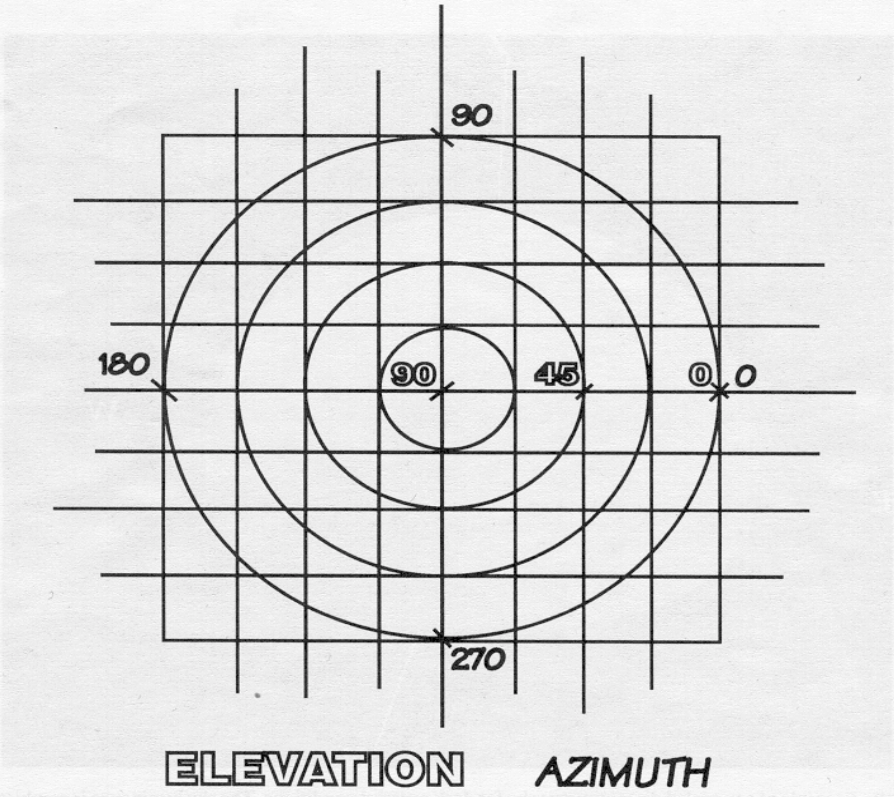

Fig. 8. Projection of the sky hemisphere on a plane used for the recursive luminance assignment process.

vations: (a) the slope of a variogram near the origin has been related to the fractal dimension[14]of the considered structure[15]and, (b) the fractal dimension of clouds has been reported to be unique and independent of sky conditions[16].

3. MODELING OF CLOUD RANDOM EFFECTS

We describe a method to incorporate the discontinuous features described above as an option to our all-weather luminance model[1]. Note that this methodology is directly applicable to any other luminance models[8,17–21]. The governing equation for the continuous luminance model is:

$$lv(\zeta, \gamma) = (1 + \alpha_1 \exp(\alpha_2/\cos\zeta))(1 + \alpha_3 \exp(\alpha_4\gamma) + \alpha_5 \cos^2\gamma) \quad (1)$$

where $lv(\zeta, \gamma)$ is the relative sky luminance at a point of zenith angle ζ and at an angular distance γ from the sun's position, and where α_1, α_2, α_3, α_4, and α_5 are coefficients that are functions of insolation condition parameters Δ, ε, and Z given in[1]. The actual continuous luminance at point ζ-γ, Lv, is obtained from the relative luminance lv via normalization to diffuse illuminance or zenith luminance as explained in[1,5,8].

We propose to model the relative discontinuous sky luminance lv' as

$$lv'(z, \gamma) = lv(\zeta, \gamma) * \mathrm{Qvi}(\zeta, \gamma) \quad (2)$$

where $\mathrm{Qvi}(\zeta, \gamma)$ is the modeled random luminance at point (ζ, γ). Qvi is obtained by generating a random luminance sky map that has geostatistical properties representative of the considered insolation conditions, as quantified by Qvi's intensity distributions and spatial variograms. The discontinuous luminance Lv' may be obtained from the relative value lv' via normalization to diffuse illuminance as above.

The generation of a Qvi sky pattern involves two main steps:

1. *Determination of the Qvi probability density function.* Based on insolation conditions parameterized by Δ and ε (two basic inputs to the continuous luminance model as well), the Qvi intensity distribution is determined. For this purpose, linear combinations of gamma functions[22]were fitted to observed distributions for each insolation condition bin specified in Table 1. The modeled probability densities, $P(\mathrm{Qvi})$ are given by:

$$P(\mathrm{Qvi}) = (1 - a)(\mathrm{Qvi}^b \exp(-\mathrm{Qvi}/c))/(b!c^{(b+1)}) + a(\mathrm{Qvi}^d \exp(-\mathrm{Qvi}/e))/(d!e^{(d+1)}). \quad (3)$$

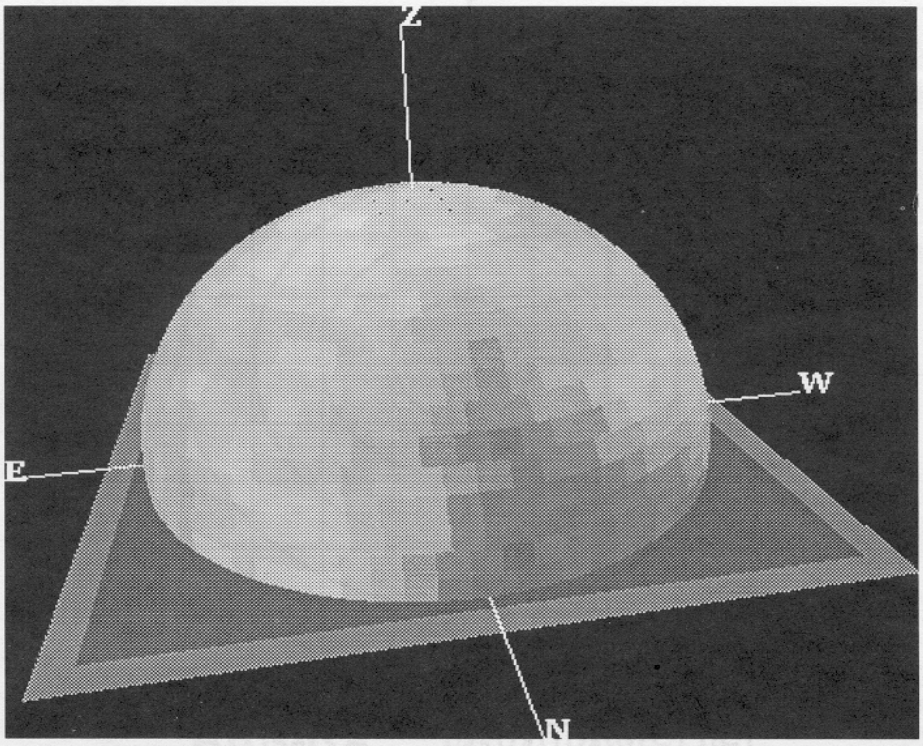

Fig. 9. Example of a modeled discontinuous sky for dark overcast conditions. The sky luminance is graphically represented by a grey scale pattern plotted on a 3-D outside view of the sky hemisphere.

The coefficients a, b, c, d, and e may be found in Table 1 for each insolation condition bin. The criterion for fitting gamma functions to experimental distributions was 1% agreement for the four first moments (mean, variance, skewness, and kurtosis). Goodness of fit may be judged qualitatively by comparing the gamma-based and actual distributions in Fig. 3.

2. *Generation of Qvi spatial distribution.* To generate a realistic spatial distribution for random luminance we propose here a simple, but effective two-dimensional recursive approach. This approach is inspired from a public domain recursive algorithm[23] which had been developed to generate cloud images on a square window. The simple structure of the recursive function allows us to incorporate both the spatial (variogram) and statistical (gamma distributions) components of the random luminance in the mapping of a random sky. This type of recursive fractal generating approach is thoroughly described in[24]along with other recursive techniques that may be applicable to this problem.

The process is first described in a simple two-dimensional representation before describing its adaptation to an hemispherical representation of the sky.

The recursive process begins by picking the four corners of a square area and assigning random values to these four points—in the present case, the random numbers, picked between 0 and 10, have probabilities assigned by the gamma distribution from step 1.

The original square is then divided into four squares as shown in Fig. 7, and values are assigned to the five newly created points as follows: the value assigned to any of the four side points is either (a) a random number (drawn from the corresponding gamma distribution) if the distance d between the considered point and its two neighboring corners is above a given threshold value L or (b) the sum of the average between the two neighboring corners and a random component x, obtained from $[x = d/L(y - 1)]$, where y is a random number drawn from the corresponding gamma distribution. The value assigned to the center of the original square is derived in a similar fashion, but using the four newly created side points instead of two neighboring corners as reference (random pick between any of the side points). The recursive process continues by subdividing each newly created square into four more squares and so on until a user-selected limit size is achieved.

In the case of the sky hemisphere, the two-dimensional approach described above incorporates the following elements.

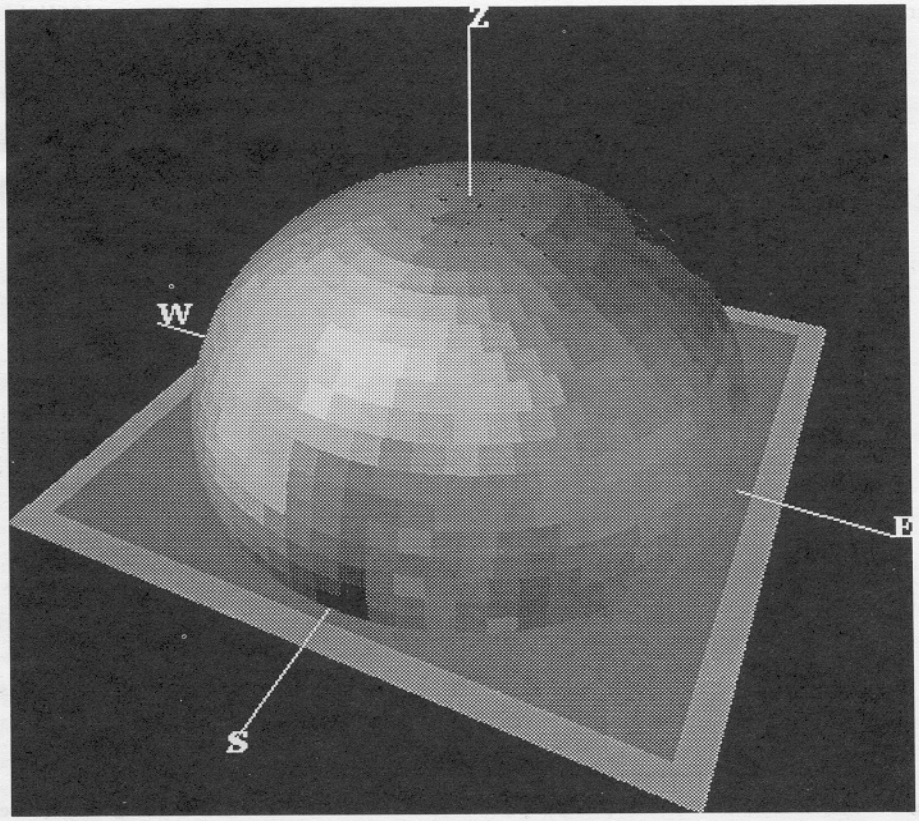

Fig. 10. Projection of the sky hemisphere on a plane used for the recursive luminance assignment process for intermediate (partly cloudy) conditions.

1. The sky hemisphere is projected on a two-dimensional plane as shown in Fig. 8, so the recursive process may take place as above in a two-dimensional imbricated square pattern;
2. the circular hemisphere's projection is inscribed into the first recursive square;
3. the distances d between two points in the recursive process are the actual (*unprojected*) angular distances between these points in the sky hemisphere;
4. the threshold distance L is taken equal to the range of the experimental variograms discussed above, estimated here at 65°; and
5. once the two-dimensional recursive process is complete, a sky map of the desired grid side is generated by transferring the two-dimensional square grid image to an equi-solid angle grid on the sky hemisphere. The resolution of this grid is selected by the user. For now, since this work is based on an experimental resolution of ten degs., we recommend that this be the working resolution of the model.

Three examples of skies generated by superimposing a modeled random sky on the continuous model patterns are given in Figs. 9, 10, and 11. As in Fig. 1, the generated sky luminance is represented by a grey scale pattern plotted on a three-dimensional sky hemisphere. These three examples correspond respectively to dark overcast, partly cloudy, and clear skies. An example overcast sky generated with a high angular resolution that illustrates the capabilities of the method, is provided in Fig. 12 (although at this time we cannot recommend such high resolution skies because of the limited resolution of this study's experimental evidence).

4. CONCLUSIONS

We have investigated the discontinuous aspects of skylight, created by "one of a kind" cloud patterns. Based on a large experimental sky scan database, we have shown that random luminance, defined as the relative difference between actual sky luminance and the modeled continuous luminance for the corresponding conditions, has predictable physical characteristics that can be parameterized as a function of insolation conditions.

We presented a simple method for incorporating these random but predictable luminance effects as an option in continuous skylight distribution models. This option should add versatility to the tools available to the daylighting design community.

As much as there is a need to validate/refine our recent all-weather continuous luminance distribution model with experimental data from other sites, it is essential to investigate whether the proposed parameterization of random luminance is a valid one for other climatic environments, and if needed, refine/upgrade this parameterization. The International Daylighting Measurement Program[25]initiated by the

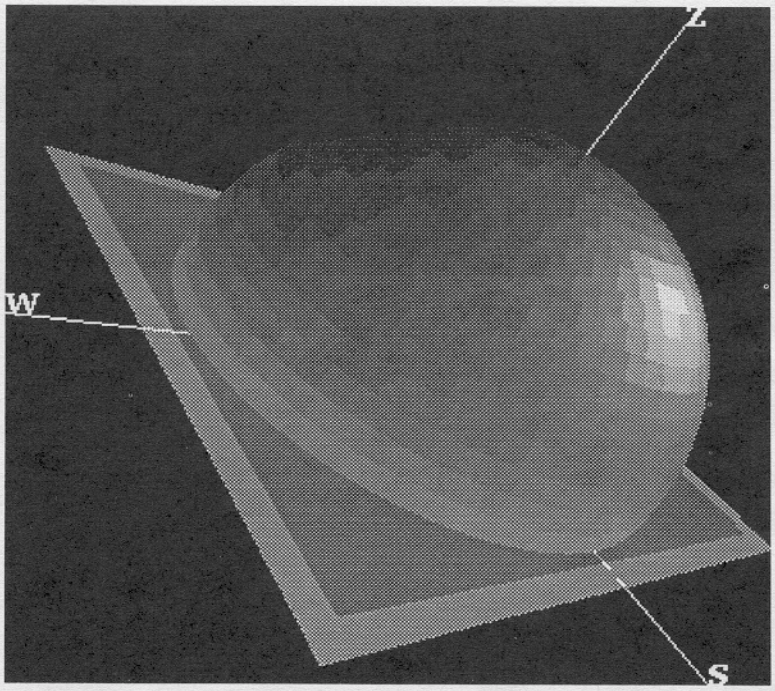

Fig. 11. Projection of the sky hemisphere on a plane used for the recursive luminance assignment process for clear conditions.

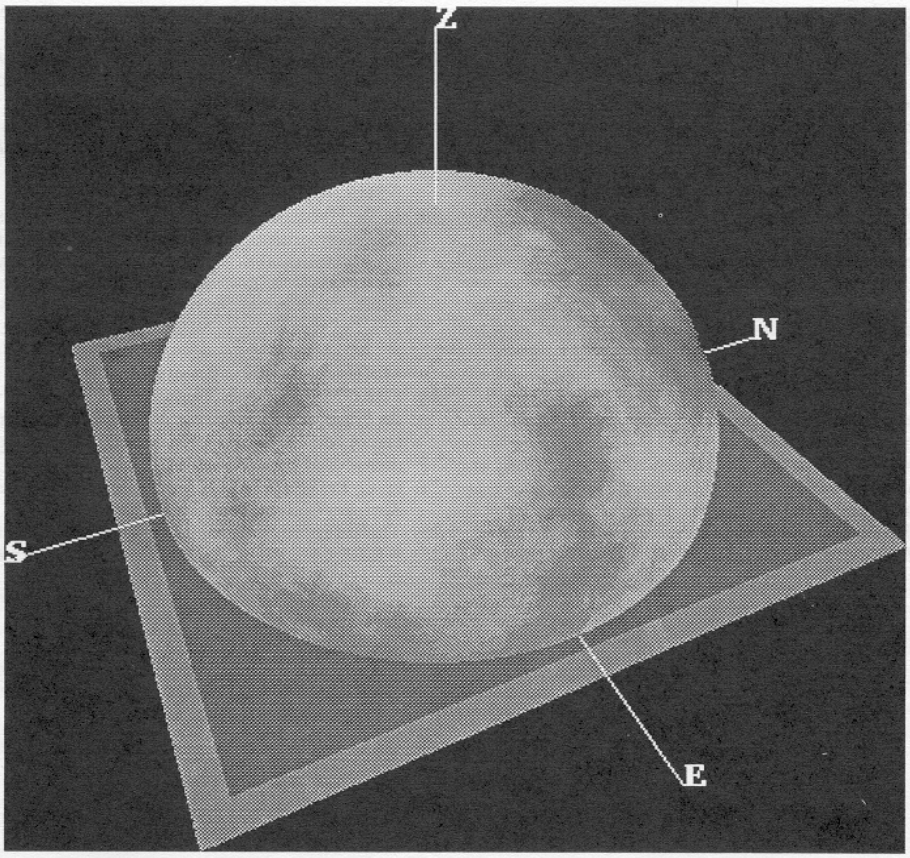

Fig. 12. Projection of the sky hemisphere on a plane used for the recursive luminance assignment process for high angular resolution.

CIE, should provide the climatically diverse data needed for this purpose.

Beyond the validation/refinement of these results, which are needed for applications in the field of daylighting, it would also be worthwhile, for those interested in cloud parameterization (e.g., for global environmental purposes), to pursue these follow-up studies: (a) investigate higher resolution sky images with a similar approach to study the behavior of spatial variograms near their origin, and (b) extrapolate the present parameterization to the analysis of satellite cloud cover images for the purpose of better predicting/forecasting insolation and daylight where this is not measured.

Acknowledgment—This work was supported by the U.S. National Science Foundation under grant #MSM 8915165. Collaboration with University of Geneva was possible thanks to support by the U.S. National Science Foundation (Grant # INT 9002363), the Swiss and U.S. DOEs' (NREL) support of the International Energy Agency SHCP Task 17-E, and the CIE/WMO's International Daylighting Measurement Program. Many thanks to Nancy Ruck (U. New South Wales) and Vito D'Agostino (Tecnopolis) for their comments and to the Mobil Foundation for enhancing these exchanges.

REFERENCES

1. R. Perez, R. Seals, and J. Michalsky, All-weather model for sky luminance distribution—Preliminary configuration and validation, *Solar Energy* **50,** 235–245 (1993).
2. M. Fontoynont, P. Barral, and R. Perez, Indoor daylighting frequencies computed as a function of outdoor solar radiation data, 22*nd CIE Conference,* Melbourne, Australia. Div. 3, pp. 100–105 (1991).
3. Y. Uetani and K. Matsuura, A mathematical model of the reflected directional characteristics for the luminance calculation in a non-isotropic diffuse reflecting interior, 22*nd CIE Conference,* Melbourne, Australia. Div. 3, pp. 94–99 (1991).
4. M. Nagata, Monte Carlo simulation of illuminance distribution and luminous flux density in interior space evenly divided by many transparent partitions, 22*nd CIE Conference,* Melbourne, Australia. Div. 3, pp. 63–64 (1991).
5. R. Perez, J. Michalsky, and R. Seals, Modeling sky luminance angular distribution for real sky conditions; experimental evaluation of existing algorithms, *Proc. of ISES World Congress,* Denver, CO, pp. 1049–1054 (1991).
6. E. Englund and A. Sparks, Geostatistical environmental assessment software, *EPA/600/4-88/033a.* Environmental Protection Agency, Washington, DC (1988).
7. A. Zelenka, G. Czeplak, V. D'Agostino, W. Josefsson, E. Maxwell, and R. Perez, International Energy Agency solar heating and cooling program, *Final Report Task 9-D,*

Solar radiation and pyranometric studies: Network supplementing techniques, Vol. 2: Theory, IEA, Paris (1992).
8. R. Perez, P. Ineichen, R. Seals, J. Michalsky, and R. Stewart, Modeling daylight availability and irradiance components, *Solar Energy* **44,** 271–289 (1990).
9. R. Perez, P. Ineichen, E. Maxwell, R. Seals, and A. Zelenka, Dynamic global-to-direct irradiance conversion models, *ASHRAE Transactions,* Vol. 98, Part 1 (1992).
10. F. Kasten and A. Young, Revised optical air mass tables and approximation formula, *Applied Optics* 28 **22,** 4735–4738 (1989).
11. Lawrence Berkeley Labs., Windows and daylighting group, LBL, Berkeley, CA.
12. E. W. Kleckner and J. J. Michalsky, A multipurpose computer-controlled scanning photometer, *PNL*-4081, Pacific Northwest Lab., Richland, WA (1981).
13. P. Moon and D. Spencer, Illumination from a nonuniform sky, *Illuminating Engineering* **37,** 707–726 (1942).
14. B. B. Mandelbrot, *The fractal geometry of nature,* W. H. Freeman and Co., New York (1982).
15. R. Bruno and G. Raspa, Geostatistical characterization of fractal model of surfaces, University of Rome, "La Sapienza," Rome, Italy (1990).
16. F. R. Cahalan and J. H. Joseph, Fractal statistics of cloud fields, *Monthly Weather Review* **117,** 261–272 (1989).
17. A. P. Brunger, The magnitude, variability, and angular characteristics of the shortwave sky radiance at Toronto, Ph.D. thesis, Univ. of Toronto (1987).
18. M. Perraudeau, Luminance models, *National Lighting Conference and Daylighting Colloquium,* Robinson College, Cambridge, U.K. (1988).
19. R. Kittler, Luminance models of homogeneous skies for design and energy performance predictions, *Proc. 2nd International Daylighting Conference,* Long Beach, CA, ASHRAE, Atlanta, GA (1986).
20. A. W. Harrison, Directional luminance versus cloud cover and solar position, *Solar Energy* **46,** 13–20 (1991).
21. K. Matsuura and T. Iwata, A model of daylight source for the daylight illuminance calculations on the all weather conditions, In: A. Spiridonov (ed.), *Proc. 3rd Int. Daylighting Conference,* NIISF, Moscow, USSR (1990).
22. A. M. Mood, *Introduction to the theory of statistics,* McGraw-Hill Book Company, New York (1950).
23. FRACTINT (Stone Soup Group), FRACTINT MS-DOS program, made available as freeware on Compuserv, Internet, etc. Original "Plasma Clouds" from a program distributed by Bret Mulvey (1992).
24. H. O. Peitgen and D. Saupe, *The science of fractal images,* Springer-Verlag, Inc., New York (1988).
25. The International Daylighting Measurement Program—IDMP, CIE, Wien, Austria and WMO, Geneva, Switzerland (1991).